Intelligent Automation And Soft Computing, 2019

Vol. 25, no. 2, 405–411
https://doi.org/10.31209/2019.100000102

# Numerical Analysis of Pressure Distribution in a Brush Seal Based on a 2-D Staggered Tube Banks Model

**Yuchi Kang[1,2], Meihong Liu[1], Sharon Kao-Walter[2,3], Jinbin Liu[1], Qihong Cen[4]**

1. Faculty of Mechanical and Electrical Engineering, Kunming University of Science and Technology, Kunming, China
2. Department of Mechanical Engineering, Blekinge Institute of Technology, SE-37179, Karlskrona, Sweden
3. College of Engineering, Shanghai Polytechnic University, Shanghai, China
4. Faculty of Materials Science and Engineering, Kunming University of Science and Technology, Kunming, China

**ABSTRACT**
A two-dimensional model of staggered tube banks of the bristle pack with different pitch ratios was solved by computational fluid dynamics (CFD). The pressure distribution along the gap centerlines and bristle surfaces were studied for different upstream pressure from 0.2 to 0.6MPa and models. The results show that the pressure is exponentially rather than strictly linearly decreasing distributed inside the bristle pack. The pressure distribution is symmetry about the circle's horizontal line. The most obvious pressure drop occurred from about 60° to 90°. There is no stationary state reached between the kinetic energy and the static pressure when the upstream is larger than 0.3MPa.

**KEY WORDS**: Brush seal, Computational Fluid Dynamics (CFD), Pressure distribution, Staggered tube banks

## 1 INTRODUCTION

A lot of researchers have demonstrated that the excellent performance of brush seals over the traditional labyrinth seals. Hence the brush seal has been employed in turbomachinery such as steam turbines and gas turbines to improve the management of secondary air system flows.

A conventional brush seal consists of thousands of bristles, which are glued or welded to a front plate and back plate. Bristles are made by Haynes25 or non-metallic materials such as Kevlar and carbon fiber.

In the past 20 years, researchers all over the world have done too much work on brush seal. Some works about tip force evaluation have been done. Li, et. al. (2012) analyzed the contact force between a single bristle and a rotor as well as a bristle pack and the rotor in an analytical way. Demiroglu, et. al. (2007) studied the tip force between bristles and the rotor by experiments. Obvious hysteresis loop could be observed and was independent with the loading rates. Bidkar, et. al. (2012) demonstrated the brush seal stiffness and hysteresis in the presence of a pressure loading. Similar curves but different in shapes were observed compared with hysteresis loop without pressure.

Flow characteristics in brush seals have been analyzed as well by many researchers. Braun and Kudriavtsev (1993) presented an analysis and numerical simulations of flow with different pitch-to-diameter-ratio (PTDR) values. In the model of PTDRL and PTDRT =1, the recirculation zones were formed in the wake of bristles. In the wake of last bristles, the shedding of eddies as well as the formulation of steady recirculation zones could be observed. Dai and Liu (2011) analyzed the fluid flow in a compact staggered tube array. They argued that the vortices generated at the bristle downstream area blocked the fluid flow and increased the pressure differential. Huang, et. al. (2016) modeled closed staggered tube banks with different pitch ratios. The pressure and velocity distribution were studied. The pressure went down first and recovered to some extents while the velocity decreased first and increased. Determine the pressure drop in a brush seal is a foundational but significant issue. Tan, et. al. (2017) analyzed the flow separation point by tube bank model.

Kang, et. al. (2018) investigated the flow resistance of brush seals by a two-dimensional model.

In this work, a two-dimensional model of staggered tube banks of the bristle pack with different ratios was

CONTACT Meihong Liu ✉: Meihong Liu,64115737@qq.com

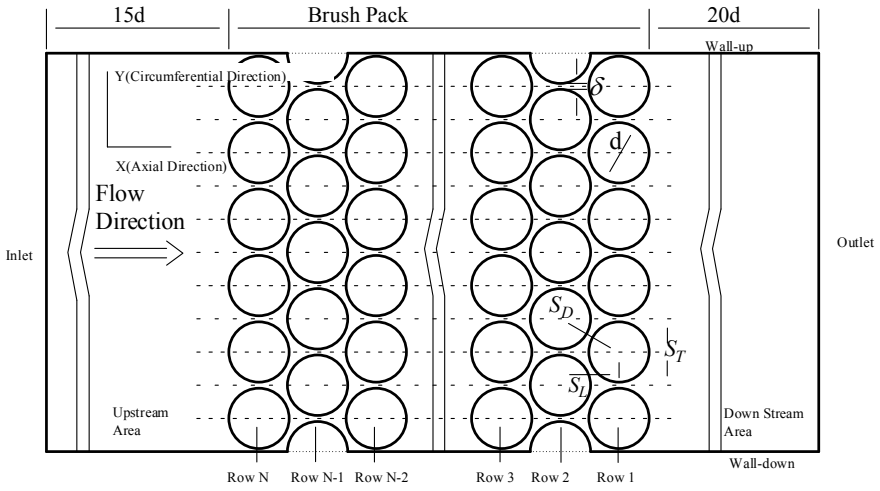


**Figure 1.** **Cross-section view of the tube banks model of brush seal.**

solved by computational fluid dynamics (CFD). This paper proceeds as follow. Section 2 focuses on the CFD simulation including the geometry, mesh, governing equations and boundary conditions. Section 3 presents the simulation results including the model verification, pressure distribution in a brush pack and around a bristle. Section 4 is the conclusions.

## 2 NUMERICAL MODELS

### *2.1 CFD model: computational domain*

FIGURE 1 presents the configuration of the cross section adopted in the computational domain. The bristles are arranged with a pitch to diameter ratio, $S_D/d$=1.05/1.1/1.12 with the diameter of 0.07mm in each model. There are 15 and 6 rows in the axial and circumferential directions, respectively. As shown in Figure 1, half tubes were also mounted along the top and bottom walls of the computational model alternately to simulate more actual arrangement. The origin of the coordinate system is defined to be at the bottom left corner. Here, the axial and circumferential directions are donated by x and y, respectively.

The geometry parameters are expressed in the followings:

$$S_D = S_T = d + \delta \tag{1}$$

$$S_L = \frac{\sqrt{3}}{2}(d + \delta) \tag{2}$$

where $S_D$ is the diagonal pitch; $S_T$ is the transverse distance between two bristles; $S_L$ is the longitudinal distance between two bristles; $\delta$ is the bristle gap.

### *2.2 CFD model: mesh generation and optimization*

Due to the compacted model, a fine mesh should be used to investigate fluid flow among the bristles. An inflation tool was used to generate 4 layers of quadrilateral cells in contact with bristle surfaces. The rest flow domain among bristles was meshed into triangular cells. Both upstream and downstream area were meshed into quadrilateral cells.

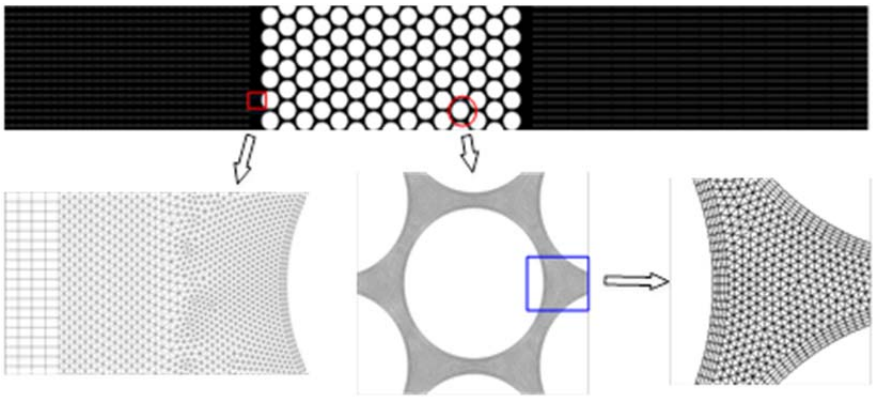

**Figure 2.** **The mesh grid for turb banks.**

### 2.3 CFD model: governing equations

The air flow is assumed to be turbulent following turbulent model. Huang, et. al. (2016), Dogu and Aksit (2006) and Sun, et. al. (2016) argued that flow is turbulent. The continuity equation, Naiver-Stokes equations for the steady flow can be expressed as followings:

Continuity equations:

$$\frac{\partial(\rho u)}{\partial x}+\frac{\partial(\rho v)}{\partial y}=0 \tag{3}$$

Naiver-Stokes equations:

$$\frac{\partial(\rho uu)}{\partial x}+\frac{\partial(\rho uv)}{\partial y}=\frac{\partial p}{\partial x}+\frac{\partial}{\partial x}\left\{\mu\left[2\frac{\partial u}{\partial x}-\frac{2}{3}\left(\frac{\partial u}{\partial x}+\frac{\partial v}{\partial y}\right)\right]\right\}+\frac{\partial}{\partial y}\left[\mu(\frac{\partial u}{\partial y}+\frac{\partial v}{\partial x})\right] \tag{4}$$

$$\frac{\partial(\rho uv)}{\partial x}+\frac{\partial(\rho vv)}{\partial y}=\frac{\partial p}{\partial y}+\frac{\partial}{\partial y}\left\{\mu\left[2\frac{\partial v}{\partial y}-\frac{2}{3}\left(\frac{\partial u}{\partial x}+\frac{\partial v}{\partial y}\right)\right]\right\}+\frac{\partial}{\partial x}\left[\mu(\frac{\partial u}{\partial y}+\frac{\partial v}{\partial x})\right] \tag{5}$$

where $p$ is the pressure of the air; $\rho$ and $\mu$ are the density and viscosity, respectively; $u$ and $v$ stand for the axial and circumferential velocity, respectively. The k-ε turbulent model is used in the present simulation along with standard wall treatment. The k-ε turbulent model is the simple and completed form of two equation Reynolds-averaged Naiver-Stoke (RANS) based turbulence model. The turbulent kinetic energy (k) and the dissipation rate (ε) can be expressed as followings:

$$\rho u\frac{\partial k}{\partial x}+\rho v\frac{\partial k}{\partial y}=\frac{\partial}{\partial x}\left[\left(\mu+\frac{\mu_t}{\mathrm{Pr}_t}\right)\frac{\partial k}{\partial x}\right]+\frac{\partial}{\partial y}\left[\left(\mu+\frac{\mu_t}{\mathrm{Pr}_t}\right)\frac{\partial k}{\partial y}\right]+G_k-\rho\varepsilon \tag{6}$$

$$\rho u\frac{\partial \varepsilon}{\partial x}+\rho v\frac{\partial \varepsilon}{\partial y}=\frac{\partial}{\partial x}\left[\left(\mu+\frac{\mu_t}{\mathrm{Pr}_t}\right)\frac{\partial \varepsilon}{\partial x}\right]+\frac{\partial}{\partial y}\left[\left(\mu+\frac{\mu_t}{\mathrm{Pr}_t}\right)\frac{\partial \varepsilon}{\partial y}\right]+C_{1\varepsilon}\frac{\varepsilon}{k}G_k-C_{2\varepsilon}\rho\frac{\varepsilon^2}{k} \tag{7}$$

where $G_k$ is the turbulent kinetic energy generated by mean velocity gradients; $\mathrm{Pr}_t$, the wall Prandtl number, is 0.85; $C_{1\varepsilon}$ and $C_{2\varepsilon}$ are 1.44 and 1.92, respectively. $\mu_t$ is the turbulent viscosity which is expressed as followings:

$$\mu_t=\rho C_\mu\frac{k^2}{\varepsilon} \tag{8}$$

### 2.4 CFD model: Boundary conditions

The appropriate initial and boundary condition are important for CFD simulations. The inlet and outlet conditions were pressure inlet and outlet. The inlet pressure was 0.2 MPa, 0.3 MPa, 0.4 MPa, 0.5 MPa and 0.6MPa, respectively. The outlet pressure was 0.1MPa. As for wall-up, wall-down and bristles, a no-slip BC was adopted. The idealized gas was assumed in the present research.

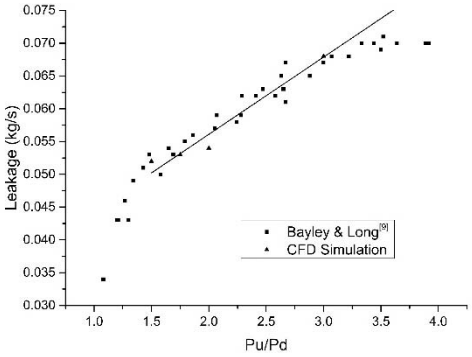


**Figure 3. Comparison of leakage for experimental and CFD result.**

## 3 RESULTS AND ANALYSIS

### 3.1 Model verification

FIGURE 3 presents the validation results of leakage. The CFD simulation results compared with previous experimental results from Bayley and Long (1992). There was an interference fit between the brush seal and the rotor with 0.25mm in the experiment. Although clearance or interference fit was not considered in the present simulation, there is a good agreement between the experiment and simulation results to some extents.

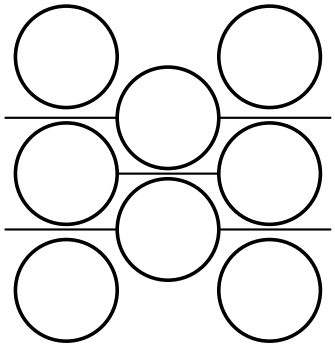

**Figure 4. Gap centerlines.**

### 3.2 Pressure distribution in a bristle pack

Ordinarily, researchers such as Huang, et. al. (2016) and Paul, et. al. (2007) analyzed the velocity and pressure distribution at gap centerlines in tube banks model. This part takes each gap centerlines in bristle pack as the research object, as shown in Figure 4, whose pressure distribution is regarded as the pressure distribution in a bristle pack. Figure 5 shows

the pressure distribution on each gap centerline with $S_D/d=1.1$ at upstream pressure 0.2MPa. The fitting formulas for upstream pressure 0.3~0.6MPa are expressed as follows:

0.3MPa: $Y=0.00628+0.03483\times0.49135^x$

0.4MPa: $Y=0.0081+0.15977\times0.26855^x$

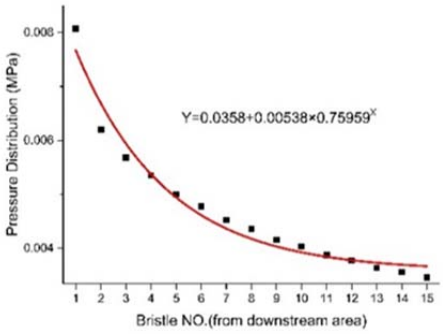


**Figure 5. The pressure distribution in a brush pack at upstream pressure from 0.2MPa.**

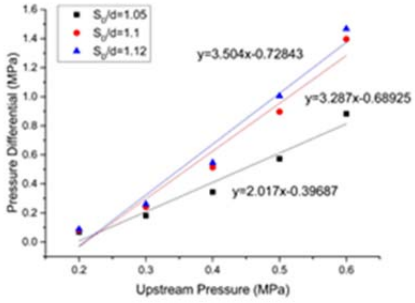


**Figure 6. The pressure distribution in a brush pack at upstream pressure 0.6MPa.**

0.5MPa: $Y=0.092+0.51948\times0.15457^x$

0.6MPa: $Y=0.00993+0.132062\times0.09819^x$

It can be clear seen that pressure is exponentially rather than linearly decreasing distributed in the bristle pack. The pressure exerted on each bristle increases with respect to bristle NO. from upstream to downstream in most cases. All the fitting curves and formulas are shown as well. One can find that the base values decrease when the upstream pressure increases. A lower base value means a more significantly steep curve which demonstrates that the uneven pressure distribution is more obvious with a higher upstream pressure. Table 1 presents the base value of fitting curves for different models and upstream pressures. At a certain upstream pressure, the base value increases with a more compact model, especially for a larger pressure differential. As for 0.2MPa, the base values for $S_D/d=1.05$ is 1.14 times as that for $S_D/d=1.1$. While for 0.6MPa, the base values for $S_D/d=1.05$ is 4.05 and 6.62 times as that for $S_D/d=1.1$ and 1.12, respectively. It can be drawn that increasing the density is an effective way to make the pressure distribution even in a large pressure differential.

**Table 1. The base values of fitting curves for different models and upstream pressures**

| Upstream pressure (MPa) | $S_D/d$ | | |
|---|---|---|---|
| | 1.05 | 1.1 | 1.12 |
| 0.2 | 0.86531 | 0.75959 | 0.64249 |
| 0.3 | 0.77116 | 0.49135 | 0.33696 |
| 0.4 | 0.67041 | 0.26855 | 0.17756 |
| 0.5 | 0.54238 | 0.15457 | 0.09096 |
| 0.6 | 0.39718 | 0.09819 | 0.06038 |

It's interesting to notice the 1st bristle, whose pressure differential is 1.3, 2, 3, 4. 5, 7 times as much as the 2nd bristle when the upstream pressure is from 0.2MPa to 0.6MPa, respectively. Such a huge loading exerted on a bristle may cause friction and wear between the 1st bristle and back plate. Especially for the upstream pressure 0.6MPa, the 1st bristle is subjected to almost 0.09MPa, which equals to a whole brush pack in a less severe working condition. Figure 6 shows the 1st bristle pressure differential with three different pitch to diameter ratios. One can discover that the 1st bristle is subjected to a larger pressure differential with a higher pitch to diameter ratio. The pressure differential goes up with respect to the total pressure differential. The slopes of the three curves are 2.017, 3.287 and 3.504, respectively. The conclusion can be drawn that the pressure differential of the 1st bristle is less sensitive to the changes of the total pressure differential with a denser brush pack.

### *3.3 Pressure distribution around a bristle*

Fluid flow across a bristle pack can be simplified to a flow across a tube banks to some extents. The main difference is the pressure differential exerted on the bristles. The analysis of the pressure distribution around a circle is a basic research. Figure 7 shows the pressure distribution along the 8th bristle at upstream pressure 0.3MPa. One can find that the pressure distribution is symmetry about the horizontal line. So the upper semicircle was analyzed in the following. There are two types of pressure distribution, which are favorable pressure gradient region ( $\partial p/\partial\theta<0$) and adverse pressure gradient region ( $\partial p/\partial\theta>0$ ), respectively. In the favorable pressure gradient region, the fluid particles in the boundary layer speed up. However, the velocity decreases in the adverse pressure gradient region. Figure 8 (a to c) show the pressure distribution along from the 15th to first bristle at upstream pressure 0.3MPa. For each bristle, A and B is the favorable pressure gradient region and C is the adverse pressure gradient region. Pressure decreases in Region A less significantly than Region B. Especially for 15th bristle, the curve is almost flat in Region A. In the Region B, θ ranges around from 62° to 95°, the pressure drop is obvious. Partially because

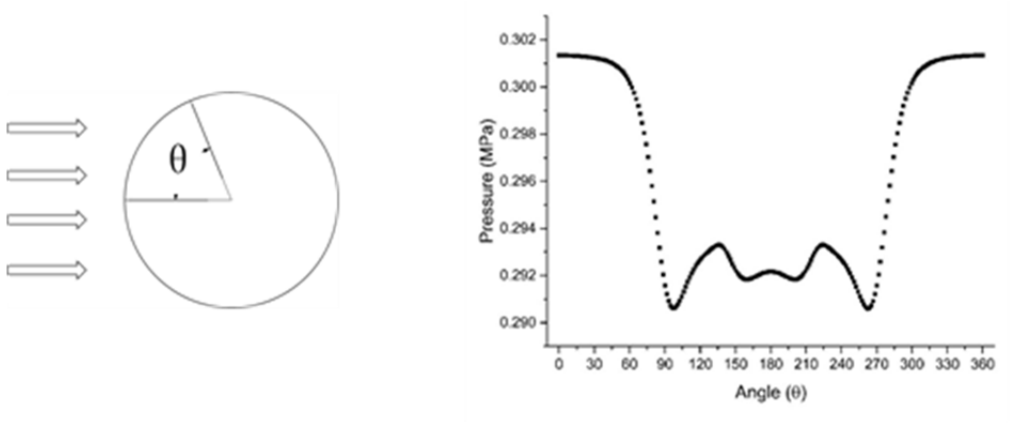


**Figure 7. The pressure distribution of 15th bristle at upstream pressure 0.3MPa**

the gap among the bristles of Region B is more narrow than the Region A and the velocity in the Region B is larger than that in the Region A, which is associated with the geometry model. Bernoulli's principle states that an increase in the speed of a fluid occurs simultaneously with a decrease in pressure, regardless of the potential term. Region C is the adverse pressure gradient region. As seen in Figure 7 and Region C in Figure 8, the pressure increases first then decreases. While there is a slight difference for the first bristle, the pressure increases slightly which is similar to a flow across a cylinder. The pressure coefficient Cp is the ratio of pressure forces to inertial forces and can be expressed as followings:

$$C_P = \frac{p(\theta) - p(0)}{0.5 \times \rho \times u_f^{\ 2}} \tag{10}$$

where p(0) is the pressure at θ=0, $u_f$ is the freestream velocity. However, it's impossible to find a $u_f$ in a tube banks models which can apply for each bristle. The local pressure coefficient is defined by Beale and Spalding (1999):

$$C_{pl} = 1 - \frac{p(0) - p(\theta)}{0.5 \times \rho \times u_m^2} \tag{11}$$

where $u_m$ is the velocity at the minimum cross section. One can discover that both $C_p$ and $C_{pl}$ reflect the relationship between static pressure energy and kinetic energy.

Figure 9 shows the Cpl of 8th bristles at a different upstream pressure from 0.2MPa to 0.6MPa. In the region A and B, Cpl decreases which means static pressure energy is converted to kinetic energy. The higher upstream pressure is, the lower Cpl is. That's to say more static pressure energy is converted to the kinetic energy. In the rear part of the bristle, Cpl varies a little and approximately equals to the minimum for upstream pressure 0.2MPa and 0.3MPa. As for 0.4MPa to 0.6MPa, Cpl fluctuated relatively obviously and the difference between Cpl at the rear part and the minimum is larger. The kinetic energy is transformed to the static pressure again. A larger pressure differential capability is one of the aims for seal parts, which can improve the overall sealing efficiency. A lower velocity of the leakage is another aim as well in order to improve sealing effect. For 0.2MPa and 0.3MPa, there is a stationary between the static pressure and the kinetic energy at the rear part. There is a certain pressure descending for a bristle seal. If a bristle seal was subjected to a more pressure differential than the critical value, more energy would transform to kinetic energy and the fluid with higher kinetic energy flee to the downstream which may increase the leakage. This is not an efficient way when installing a brush seal in a turbomachinery. It's better to adopt a multi-stage brush seal when the pressure differential is larger than 0.3MPa. This conclusion is similar to previous actual experience by Zhu (2012).

Figure 10 shows the $C_{pl}$ at upstream pressure 0.3MPa with different spacings. As for the $S_D/d$=1.1 and 1.12, there is a slight difference between the two and $C_{pl}$ of $S_D/d$=1.1 is a little bit lower than $S_D/d$=1.12. Both the minimum are around -2 and they change less significantly than the front part. For the spacing of 1.05, there is a huge difference with the other two. $C_{pl}$ goes down first and recovers a little then decreases again to its minimum, at around -12, which means the kinetic energy is transformed to the pressure energy. The Region C is different with the other two in shape. The preliminary reason for this is that the denser tube bank has a better block effect on the fluid flow then the pressure drop is larger than the other two arrangements.

## 4 CONCLUSION

TO clarify the pressure distribution in a brush pack, CFD simulations were conducted by three staggered tube banks models with five different upstream pressure. The pressure distribution inside a bristle

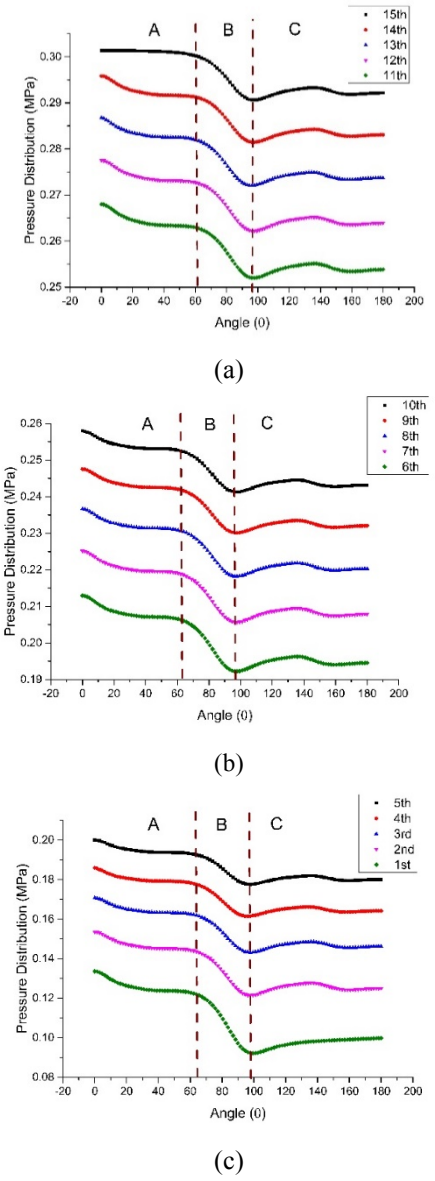


**Figure 8.** The local pressure coefficient of 8th Bristle at upstream pressure from 0.2MPa to 0.6MPa.

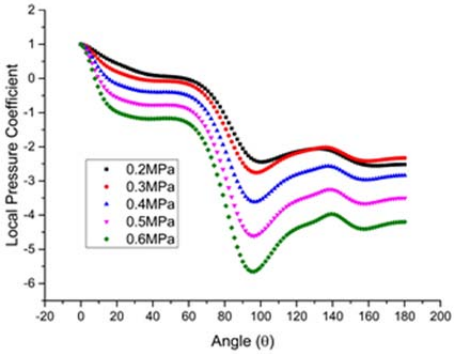


**Figure 9.** The pressure distribution of 15th bristle at upstream pressure 0.3MPa.

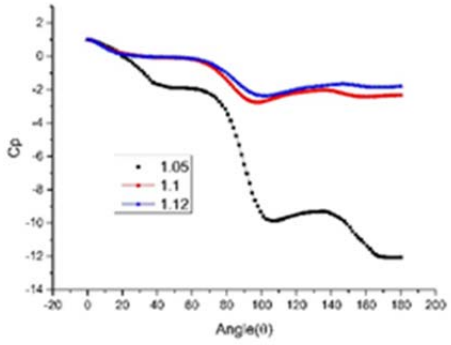


**Figure 10.** The local pressure coefficient of 8th bristle at upstream pressure 0.3MPa with different spacings.

pack and along a bristle were analyzed. The main results are summarized as follows:

1. The pressure is exponentially rather than strictly linearly decreasing distributed in the bristle pack. Under a larger pressure differential, the uneven pressure distribution is obvious. The base values increase obviously in a denser bristle pack which means it's more efficient to arrange a denser bristle pack in a higher pressure differential.

2. The first bristle is subjected to the highest pressure differential in a brush pack. The pressure differential is larger with a higher total pressure differential. Increasing a brush density is a better way to decrease the pressure differential on the first bristle.

3. The pressure distribution is symmetry about the circle's horizontal line. The most obvious pressure drop occurred from about 60° to 90°, which may be associated with the geometry arrangement.

4. The local pressure coefficient $C_{pl}$ can reflect the relationship between the static pressure and the kinetic energy of a brush pack. When the upstream is smaller than 0.3MPa, a balance reached between the static pressure and the kinetic energy. It's better to adopt a multi-staged brush pack in a larger pressure differential working conditions.

## 5 REFERENCE

F. J. Bayley and C. Long. (1992). A Combined Experimental and Theoretical Study of Flow and Pressure Distributions in a Brush Seal. *ASME 1992 International Gas Turbine and Aeroengine Congress and Exposition*.

S. B. Beale and D. B. Spalding. (1999). A Numerical Study OF Unsteady Fluid Flow in In-line and Staggered Tube Banks. *Journal of Fluids and Structures*, 13(6), 723-754.

R. A. Bidkar, X. Zheng, M. Demiroglu, et al. (2011). Stiffness Measurement for Pressure-Loaded Brush Seals. *ASME 2011 Turbo Expo: Turbine Technical Conference and Exposition*, 789-796.

M. J. Braun and V. V. Kudriavtsev. (2008). A Numerical Simulation of a Brush Seal Section and

Some Experimental Results. *Journal of Turbomachinery*, 117(1), 190-202.

W. Dai, and Y. Liu. (2011). Numerical simulation of fluid flow across compact staggered tube array. *Manufacturing Automation*, 33(1), 107-110.

M. Demiroglu, M. Gursoy and J. A. Tichy (2007). An Investigation of Tip Force Characteristics of Brush Seals. *ASME Turbo Expo 2007: Power for Land, Sea, and Air,* (pp. GT2007-28042).

Y. Dogu, and M. F. Aksit. (2005). Brush Seal Temperature Distribution Analysis. ASME Turbo Expo 2005: Power for Land, Sea, and Air, 128(3), 页 1237-1248.

S. Huang, S. Suo, Y. Li et al. (2016). Flows in brush seals based on a 2-D staggered tube bundle model. *Journal of Tsinghua University (Science and Technology)*, 56(2), 160-166.

Y. Kang, M. Liu, S. Kao-Walter et al. (2018). Predicting aerodynamic resistance of brush seals using computational fluid dynamics and a 2-D tube banks model. *Tribology International*, 126, 9-15.

J. Li, J. Yang, L. Shi et al. (2012). Analytical Investigations on the Contact Force Between Bristle Packs and Shaft Surface of Brush Seals. *ASME Turbo Expo 2012: Turbine Technical Conference and Exposition*, 2211-2218.

S. S. Paul, M. F. Tachie, and S.J. Ormiston. (2007). Experimental study of turbulent cross-flow in a staggered tube bundle using particle image velocimetry. *International Journal of Heat and Fluid Flow*, 28(3), 441-453.

D. Sun, N. Liu, C. Fei, et al. (2016). Theoretical and numerical investigation on the leakage characteristics of brush seals based on fluid‐structure interaction. *Aerospace Science and Technology*, 58, 207-216.

Y. Tan, M. Liu, Y. Kang et al. (2017). Investigation into brush seal vortex separation point based on 2D staggered tube bundle model. *Journal of Drainage and Irrigation Machinery Engineering*, 35(7), 602-608.

Z. Zhu. (2005). The design and application of brush seals. *Gas Turbine Technology*, 18(3)

## 6 ACKNOWLEDGEMENT

THE current research has been supported by China Scholarship Council (granted no.201608740003) and National Natural Science Foundation of China (granted no.51765024).

## 7 DISCLOSURE STATEMENT

NO potential conflict of interest was reported by the authors.

## 8 NOTES ON CONTRIBUTORS

**Yuchi Kang** is Ph.D student at Faculty of Mechanical and Electrical Engineering, Kunming University of Science and Technology. Also, he is a visiting Ph.D student at Blekinge Institute of Technology. He focuses on brush seal and CFD application. He received BS from Liaoning University of Technology in 2013.

Corresponding Author: **Meihong Liu** received Ph.D. from East China University of Science and Technology in 2004. She is a professor in sealing technology at Faculty of Mechanical and Electrical Engineering, Kunming University of Science and Technology. Her research field includes sealing technology and multi-field coupling problems.

**Sharon Kao-Walter** received her BS from Shanghai Jiaotong University in 1982. Then she got her Licentiate Degree from Lund University of Technology in 1991 and Ph.D degree from Blekinge Institute of Technology (BTH) in 2005. She is a professor in Solid Mechanics since April 2015 at the department of Mechanical Engineering in BTH.

**Jinbin Liu** received a BS degree in Mechanical Engineering from Liaoning University of Technology, China in 2016. Currently, he is a master student at Kunming University of Science and Technology.

**Qihong Cen** received his BS and MS from Kunming University of Science and Technology in 1998 and 2001, respectively. He received his Ph.D from Xi'an Jiaotong University in 2005. He is an associate professor at Faculty of Materials Science and Engineering, Kunming University of Science and Technology.